HHS Public Access

Author manuscript

Biochemistry. Author manuscript; available in PMC 2019 April 10.

Published in final edited form as:

Biochemistry. 2018 December 18; 57(50): 6878–6887. doi:10.1021/acs.biochem.8b01032.

RNA Recognition-like Motifs Activate a Mitogen-Activated Protein Kinase

Timothy Phillips[#], **Chong Wai Tio**[#], **Gregory Omerza**, **Abhimannyu Rimal**, **Ravi K. Lokareddy**, **Gino Cingolani**, and **Edward Winter**[*]

Department of Biochemistry and Molecular Biology, Thomas Jefferson University, Philadelphia, Pennsylvania 19107, United States

[#] These authors contributed equally to this work.

Abstract

Smk1 is a mitogen-activated protein kinase (MAPK) family member in the yeast *Saccharomyces cerevisiae* that controls the postmeiotic program of spore formation. Ssp2 is a meiosis-specific protein that activates Smk1 and triggers the autophosphorylation of its activation loop. A fragment of Ssp2 that is sufficient to activate Smk1 contains two segments that resemble RNA recognition motifs (RRMs). Mutations in either of these motifs eliminated Ssp2's ability to activate Smk1. In contrast, deletions and insertions within the segment linking the RRM-like motifs only partially reduced the activity of Ssp2. Moreover, when the two RRM-like motifs were expressed as separate proteins in bacteria, they activated Smk1. We also find that both motifs can be cross-linked to Smk1 and that at least one of the motifs binds near the ATP-binding pocket of the MAPK. These findings demonstrate that motifs related to RRMs can directly activate protein kinases.

Graphical Abstract

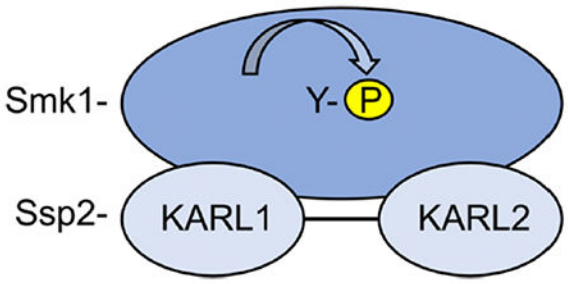

Mitogen-activated protein kinases (MAPKs) comprise a family of serine/threonine (S/T) protein kinases that transduce a broad array of signals in eukaryotic organisms. MAPKs are activated by phosphorylation of a conserved threonine (T) and tyrosine (Y) in their activation loops.[1] "Canonically" activated MAPKs are controlled by dualspecificity MAPK kinases, while "non-canonically" activated MAPKs do not use MAPK kinases and often

[*]**Corresponding Author**: Department of Biochemistry and Molecular Biology, 233 S. 10th St., Philadelphia, PA 19107. edward.winter@jefferson.edu. Telephone: (215) 503-4139. Fax: (215) 923-9162.

The authors declare no competing financial interest.

undergo autophosphorylation as part of the activation mechanism.[2,3] The autophosphorylation of MAPKs can occur in *cis* (intramolecular) or in *trans* (intermolecular). The *cis* autophosphorylation of Y residues plays a particularly prominent role in activating MAPKs and MAPK-like kinases.

While MAPKs are often assumed to be activated by a single mechanism, MAPKs such as mammalian p38 can be activated canonically in one cell type and by autophosphorylation in another.[4,5] The well-studied Fus3 MAPK is canonically activated in response to mating pheromones, yet upon activation, it further autophosphorylates its activation-loop Y to influence the output properties of the pathway.[6,7] Early studies revealed that the canonically activated Erk1 and Erk2 MAPKs from mammals can autophosphorylate their activation-loop Y residues in vitro, yet a physiological role for these reactions has not been described.[8–11] There are numerous protein kinases related to MAPKs (e.g., CDK-like kinases and GSK family members) that autophosphorylate their activation-loop Ys, yet little is known about how these reactions are controlled.[12–20] Taken together, these findings suggest that *cis* autophosphorylation of Y residues is an ancient property of MAPKs and MAPK-like kinases that has been suppressed to variable extents over evolutionary time to diversify the properties of the modern kinome.

Smk1 is a meiosis-specific MAPK from *Saccharomyces cerevisiae* that is activated by a noncanonical mechanism as cells complete nuclear segregation.[21–28] *SMK1* is controlled by a tightly regulated middle meiotic (Ndt80-inducible) promoter as cells exit meiotic G2 (prophase) and enter meiosis I (MI).[29,30] Once it is translated, Smk1 is almost immediately phosphorylated on its activation-loop T residue by the CDK-activating kinase, Cak1.[27,28] This produces the monophos-phorylated form of Smk1 that is distributed throughout the cell as MI is taking place.[25] During MII, double membranes termed prospore membranes (PSMs) surround the haploid cells.[31–33] A substantial fraction of the monophosphorylated Smk1 localizes to PSMs.[25,34]

Like *SMK1, SSP2* is a middle meiotic gene that is transcriptionally induced by Ndt80.[35] However, in contrast to *SMK1* mRNA, *SSP2* mRNA is translationally repressed until MII by the Rim4 RNA-binding protein.[25,36–39] As anaphase II is taking place, the meiosis-specific CDK-like kinase Ime2 phosphorylates Rim4, thereby translationally derepressing *SSP2* mRNA. Ssp2 protein then localizes to the PSM. In a process that is not well understood, the anaphase-promoting complex (APC) E3 ubiquitin ligase bound to a meiosis-specific substrate-bridging protein, Ama1 (a Cdc20 homologue), promotes binding of Ssp2 to Smk1. Ssp2 activates Smk1, thereby triggering the intramolecular autophosphorylation of SmkTs activation-loop Y residue to produce the fully active form of Smk1. Ime2 and Ama1 are associated with exit from meiosis II, closure of the PSM, and cellularization. These interactions have been proposed to couple completion of MII to activation of the Smk1 kinase, which then regulates late steps in the program.

In previous studies, we demonstrated that Ssp2 consists of an amino-terminal segment that targets the protein to the PSM (the targeting domain or TD is within the segment of residues 1–100).[25] The TD is not required for Smk1 activation. While *ssp2*Δ and *smk1*Δ mutants form defective spores, mutants lacking residues 1–161 of Ssp2 form spores that are

morphologically indistinguishable from wild-type spores. The carboxy-terminal segment of Ssp2 (residues 164–371) is sufficient to activate Smk1 (this segment will be termed the kinase-activating domain or KAD hereafter). In this study, we interrogated the structure–function relationships of $Ssp2^{KAD}$. We found that two modules in $Ssp2^{KAD}$ that resemble RNA recognition motifs (RRMs) are essential for Smk1 activation. RRMs are some of the most abundant motifs encoded by eukaryotic genomes. These findings expand the functional repertoire of RRM-like modules to direct activators of protein kinases.

MATERIALS AND METHODS

Yeast Strains, Bacterial Strains, Culture Conditions, and Plasmids.

All yeast strains used in this study are in the SK1 genetic background (Table 1). Yeast were grown in YPD (1% yeast extract, 2% peptone, and 2% glucose). For sporulation experiments, cells were grown overnight in YPA (1% yeast extract, 2% peptone, and 2% potassium acetate) to a density of 10^7 cells/mL. Cells were washed in sporulation medium (2% potassium acetate, 10 μg/mL adenine, 5 μg/mL histidine, 30 μg/mL leucine, 7.5 μg/mL lysine, 10 μg/mL tryptophan, and 5 μg/mL uracil), resuspended to a density of 4×10^7 cells/mL in sporulation medium, and placed on a roller drum at 30 °C for the indicated times.

Strains containing $Ssp2^{KAD}$-GST linker mutations were created by amplifying the coding sequence from plasmids pTP66, pTP67, pTP68, and pTP69 (see below) with oligonucleotides containing a 50 bp sequence of the natural *SSP2* promoter on the 5’ end. These polymerase chain reaction (PCR) fragments were combined with *GST-TRP1*[40] using overlapping PCR and transformed into JTY1016 to generate the mutated $SSP2^{KAD}$-*GST* linker mutation driven by the *SSP2* promoter. This haploid was crossed with JTY1008, and diploids were isolated.

The SK1 forms of yeast genes were used for all plasmids used in this study unless otherwise indicated. pET-Duet-derived plasmid pJT115 for expressing wild-type *SMK1* and $SSP2^{KAD}$-*GST* has previously been described.[24] Amber suppressor codons were introduced into pJT115 using site-directed mutagenesis (New England Biolabs). GST-tagged Ssp2 truncations were created by oligonucleotides annealing to the desired gene location with a 5′ NcoI site and 3′ NotI site. The truncated genes were amplified with these oligonucleotides, digested, and ligated into a similarly digested pJT115 plasmid, replacing the *SSP2*-Δ*N137*-*GST* gene. To construct the MBP-KARL1 fusion plasmids, an upstream oligonucleotide containing a NcoI restriction endonuclease site linked to the amino-terminal codons of MBP and a downstream oligonucleotide corresponding to the multicloning site of pMAL-c2x were combined with a PCR fragment encoding residues 162–265 of SSP2 that had been codon-optimized for *Escherichia coli* expression (Genscript) linked to a NotI restriction endonuclease site. This fragment was inserted into the NcoI/NotI sites of plasmid pACYC-DUET. Deletion derivatives of this plasmid were constructed similarly using oligonucleotides corresponding to the indicated regions of *SSP2* linked to a NotI site. Plasmid pTP52 with the yeast SK1 sequence encoding KARL2 was created by replacing the NheI/NotI fragment from pTP40 with the NheI/NotI fragment from pJT115 generated by

PCR using oligonucleotides containing these same sites. Mutations in the linker region of $Ssp2^{KAD}$ were created from pJT118 using site-directed mutagenesis.

Recombinant proteins were expressed in BL21(DE3) cells. Flasks containing 50 mL of LB (10% tryptone, 10% NaCl, and 5% yeast extract) and selective antibiotics (100 μg/mL ampicillin and 25 μg/mL chloramphenicol) were inoculated with an overnight starter culture. Cells were grown at 37 °C until they reached logarithmic growth phase (A_{600} of 0.6) and cooled on ice. Protein expression was induced with 500 μM isopropyl β-D-1-thiogalactopyranoside, and cells were then incubated overnight at 18 °C. For the Bpa cross-linking experiments, arabinose was also added to a final concentration of 0.2% to induce the expression of the tRNA and tRNA synthetase encoded by the pEVOL plasmid.[41]

Protein Purification and Analyses.

GST-tagged proteins were purified from bacteria and yeast as previously described.[24] SmkI-HH proteins were purified using nickel beads under denaturing conditions as previously described.[42] To analyze protein expression in total bacterial lysates, cells were collected by centrifugation and boiled in sample buffer, and 0.05 A_{600} unit was electrophoresed on denaturing polyacrylamide gels. To analyze yeast cell extracts, cells were collected and lysed with NaOH, and proteins precipitated using trichloroacetic acid as previously described.[34]

Cross-Linking.

BL21(DE3) cells containing a pET-Duet plasmid containing *SMK1* and *$SSP2^{KAD}$-GST* and the pEVOL plasmid were grown in LB medium containing antibiotics and 1 mM Bpa. Cells were induced and lysed, and the Smk1/Ssp2-GST complex was purified as described above. Proteins were eluted in 300 μL of elution buffer [500 mM Tris and 25 mM reduced glutathione (pH 8.0)] and cross-linked on ice with ultraviolet (UV) light (λ_{365}) for 1 h using a Stratalinker 1800. The sample was then diluted 1:1 with 2× sample buffer.

Electrophoresis and Immunoblot Assays.

Samples were electrophoresed through 8% polyacrylamide gels (29:1 acrylamide:bis-acrylamide) at a constant current of 45 mA. Proteins were transferred to Immobilon-P membranes and probed with the following antibodies: for Smk1 lacking an epitope tag, an affinity-purified rabbit polyclonal antibody raised against a peptide contained in the C-terminus of the protein (CLQGPFDFTYESELNSMSKLRD) at a 1:7500 dilution; for Smk1-pY209, an affinity-purified rabbit polyclonal antibody specific for phosphorylated Y209 at a 1:2000 dilution;[28] for GST, a mouse GST antibody (Santa Cruz Biotechnology) at a 1:10000 dilution for bacterial samples and a 1:500 dilution for yeast samples; for MBP, a mouse monoclonal MBP antibody (New England Biolabs) at a 1:10000 dilution; and for the HA epitope, a mouse HA.11 monoclonal antibody at a 1:10000 dillution (Berkeley Antibody Co.).

Structure Analysis.

Homology models of Smk1 and the KAD domain of Ssp2 were generated using Swiss-Model.[43] Ssp2 was modeled after the structure of polypyrimidine tract-binding protein 2

[Protein Data Bank (PDB) entry 4cq1], which is 21% identical in amino acid sequence. SmkI was modeled after ERK5 (PDB entry 5O7I), which is 41% identical in primary sequence. Secondary structure superimposition of the Fus3:Ste5 complex (PDB entry 2F49) onto Smk1 was carried out as described in Coot.[44] All ribbon diagrams were prepared using the PyMOL Molecular Graphics System. Secondary structure predictions were carried out as described by Jones.[45]

RESULTS

Ssp2^{KAD} consists of two segments that have modest sequence similarity to members of the RRM superfamily. RRMs are 70–90-amino acid segments that fold into a compact structure consisting of four antiparallel β-sheets that pack against two α-helices in a $\beta\alpha\beta\beta\alpha\beta$ topology.[46] Canonical RRMs recognize RNA via aromatic residues (usually F but sometimes Y) in ribonucleoprotein (RNP) amino acid sequence elements that are located in the first and third β-sheets. Consistent with the sequence similarity, the two Ssp2^{KAD} segments are predicted to adopt ordered $\beta\alpha\beta\beta\alpha\beta$ secondary structures (Figure 1A). However, RNP elements are not apparent in Ssp2^{KAD}, and while aromatic residues are present in the β3-sheets of both of the RRM-like segments, they are absent in the β1-sheets. Ssp2's RRM-like segments are separated by a segment that is predicted to have a low degree of sequence complexity. The data presented below will demonstrate that the RRM-like segments bind to the Smk1 MAPK, thereby activating the kinase. For the sake of simplicity, the segments will hereafter be termed kinase-activating RRM-like motifs (KARL1 and KARL2), and the segment separating the KARLs will be termed the linker (see Figure 1A).

Mutational Analyses of the KARLs Suggest Similarities to Canonical RRMs.

KARL2 contains two F residues (F307 and F327) that appear to be shared in the yeast Mrn1 and Nab6 RNA-binding proteins. We previously showed that an *ssp2-F307A,F327A* mutant fails to activate autophosphorylation of Smk1 on its activation-loop Y (Y209) and that it has an *ssp2*Δ-like phenotype in yeast (meiosis occurs, but spores are undetectable).[34] F327 is located in the β3-sheet of the predicted $\beta\alpha\beta\beta\alpha\beta$ secondary structure of KARL2 and is in a position similar to those of Fs that stack with RNA bases in canonical RRM–RNA interactions, while F307 is adjacent to α1 and does not correspond to RRM residues known to contact RNA (see Figure 1A). F211 is located in β3 of the predicted $\beta\alpha\beta\beta\alpha\beta$ secondary structure of KARL1 and is comparable to F327 (an aromatic residue in KARL1 corresponding to F307 in KARL2 is not apparent from the sequence).

Ssp2^{KAD}-GST activates Smk1 to autophosphorylate its activation-loop Y when these proteins are co-expressed in bacteria.[24] This reaction can be monitored with a phospho-specific antiserum directed against pY209 in Smk1. At least a fraction of the Ssp2^{KAD}-GST/Smk1 complex that is formed in bacteria is catalytically active against bacterial proteins, and this can be monitored using a phospho-specific antibody directed against pT. We used the bacterial co-expression system to compare the ability of the wild-type and mutant forms of Ssp2^{KAD}-GST to activate Smk1. Similar to those in yeast, the double F307A/F327A mutations in KARL2 eliminated detectable Smk1 autophosphorylation in bacteria (Figure 1B). The F307A/F327A substitutions also eliminated catalytic output of Smk1 as measured

with the pT antibody. In contrast, mutation of F307 and F327 to Ys only modestly decreased the level of Smk1 autophosphorylation and catalytic output. We tested the individual F307A and F327A mutations and found that either substitution impaired autophosphorylation of Y209 and catalytic activity for substrates. As expected from the analysis of the F307Y/F327Y double mutant, substitution of either of these residues with Y had only modest effects on autophosphorylation and substrate phosphorylation. The substitution of F211 in KARL1 with either A or Y eliminated detectable autophosphorylation and sharply decreased the level of substrate phosphorylation. Taken together, the similarity of Ssp2's amino acid sequence to RNA-binding proteins, the predicted secondary structure of KARL1 and KARL2, and the mutational data suggest that Ssp2 interacts with Smk1 through motifs that are related to RRMs. These data also indicate that residues in $\beta 3$ of the predicted $\beta\alpha\beta\beta\alpha\beta$ folds of KARL1 and KARL2, which may correspond to residues in canonical RRMs that directly contact RNA bases, are important for Ssp2's ability to activate Smk1.

KARL1 and KARL2 Expressed as Separate Proteins Can Activate Smk1.

We next tested whether KARL1 and KARL2 can activate Smk1 when expressed separately. For this purpose, maltose-binding protein (MBP) fused to the N-terminus of residues 162–265 of Ssp2 (MBP-KARL1) and GST fused to the C-terminus of residues 266–371 (KARL2-GST) were co-expressed with Smk1 in *E. coli* and Smk1 autophosphorylation was assayed. These experiments show that MBP-KARL1 and KARL2-GST expressed as separate proteins are capable of activating Smk1 autophosphorylation in bacteria (in Figure 2, compare lanes 2 and 4). To further define KARL1, amino acids in the predicted linker from MBP-KARL1 were deleted (from the carboxy terminus of the fusion protein) and these deletants were tested to determine whether they could activate Smk1 autophosphorylation when expressed with functional KARL2-GST. We also deleted residues in the predicted linker from KARL2-GST (deletions from the amino terminus of the fusion protein) and similarly tested these deletants in bacteria expressing functional MBP-KARL1. These experiments revealed that while both KARL1 and KARL2 are required to activate Smk1 autophosphorylation, they can do so when expressed separately and that residues 245–265, predicted to be in the linker, are dispensable for Smk1 activation. We previously showed that small deletions that encroach on either end of the Ssp2 fragment of amino acids 162–371 eliminated its ability to activate Smk1, thus defining the boundaries of functional $Ssp2^{KAD}$ as diagrammed in Figure 1A. Taken together, these findings demonstrate that the 84-residue segment containing KARL1 (amino acids 162–245) and the 106-residue segment containing KARL2 (amino acids 266–371) are sufficient to activate Smk1 autophosphorylation in the *E. coli* expression system. The $\beta\alpha\beta\beta\alpha\beta$ secondary elements, common to RRMs, are contained in the functional 84-residue KARL1 and the 106-residue KARL2 fragments. For KARL1, there is a close correlation between deletions that remove secondary elements and a loss of functionality (compare lanes 8 and 9 in Figure 2). This is consistent with an RRM-like fold in KARL1 being necessary and sufficient for functionality. For KARL2, the correlation between the loss of function and removal of the predicted secondary elements is not as precise. In particular, the removal of residues 266–275, which are 10 amino acids amino-terminal to the first predicted β-sheet in KARL2, eliminated function (compare lanes 4 and 5 in Figure 2). This observation suggests that a short segment within 18 amino acids of the first predicted β-sheet in KARL2 (see Figure 1A) is required for functionality. It is also

notable that MBP-KARL1 and KARL2-GST are both produced at levels higher than that of Ssp2^{KAD}-GST (based on GST immunoreactivity and total protein staining), yet more Smk1 is autophosphorylated in the Ssp2^{KAD}-GST-producing cells (compare lanes 3 and 4 in Figure 2). This finding suggests that the intact KAD is a more efficient activator of Smk1 than the separately produced KARL1 and KARL2 proteins (see Discussion).

The Linker Can Tolerate Substantial Mutation.

To further test the role of the Ssp2 linker in Smk1 activation, residues 247–256 (YENIMKEQSV) within the linker (yellow segment in Figure 1A) were duplicated, deleted, or replaced with two to five copies of an artificial linker sequence (GGGS) in the Ssp2^{KAD}-GST construct (mutants L1–L4, respectively, in Figure 3A). The wild-type *SSP2* gene was replaced with the L1–L4 derivatives in *SMK1-HH* yeast, and the phenotypes of the L mutants were tested. All of the L mutant proteins bound Smk1-HH, activated autophosphorylation (Figure 3B), and promoted spore formation (Figure 3C), but they were only partially functional in all of these assays. The L mutants therefore appear to be hypomorphic. In contrast, substitutions in KARL2 (F307A/F327A) and relatively small deletions in KARL2 (351–371Δ) or KARL1 (162–170Δ) have previously been shown to completely eliminate the ability of Ssp2^{KAD}-GST to bind Smk1-HH and activate autophosphorylation.[25,34] Moreover, the cellular phenotypes of these KARL mutants and the *ssp2*Δ phenotype were indistinguishable when tested in parallel (spore walls were not detected in any of the >300 individual cells examined for each of these KARL mutants or in the *ssp2*Δ mutant). These findings demonstrate that KARL1 and KARL2 are essential for any activity of Ssp2. In contrast, while the overall length and amino acid composition of the linker can influence Ssp2/Smk1 binding and thus Smk1 activation, the linker can tolerate substantial mutational perturbation without eliminating function.

A Residue in Smk1 near the ATP-Binding Pocket Can Be Cross-Linked to Ssp2^{KAD}.

To further interrogate the interaction of Ssp2 and Smk1, we utilized a bacterial expression strategy that incorporates non-natural cross-linkable amino acids at specific positions within a target protein.[41,47] This system utilizes an aminoacyl-tRNA synthetase that charges an engineered amber suppressor tRNA with the non-natural amino acid *p*-benzoyl-L-phenylalanine (Bpa). Upon exposure to UV light, the Bpa side chain can form covalent bonds with carbon atoms that are within 4 Å. Amber codons were introduced at various positions in a plasmid that directs the inducible expression of both *SMK1* and *SSP2^{KAD}-GST*. These plasmids and a second plasmid that directs the expression of the tRNA and synthetase were co-transformed into bacteria, and transformants were induced in medium containing Bpa. Subsequently, samples were irradiated with UV and resolved by electrophoresis in denaturing gels, and Smk1 or Ssp2 proteins detected by immunoblot analyses. If the amber suppressible residue in one of the Smk1/Ssp2^{KAD}-GST proteins is within 4 Å of a C atom of the second protein, new electrophoretic species approximating the combined masses of Smk1 and the Ssp2^{KAD}-GST complex may be detected.

We first tested whether Smk1 derivatives containing Bpa substituted at various positions could be cross-linked to Ssp2^{KAD}-GST. A complication of these experiments is that the Bpa substitution might cause misfolding of the Smk1 kinase that would prevent it from binding

Ssp2. To control for this possibility and to enrich for the cross-linked entities we hoped to detect, Smk1/Ssp2^{KAD}-GST complexes were purified using reduced glutathione prior to UV cross-linking. The ability of Smk1 to autophosphorylate Y209 served as an indicator of catalytic output. We tested a variety of substitution mutants in Smk1 that were predicted to be in regions of the kinase that are solvent-exposed and in segments of the MAPK corresponding to those known to interact with regulatory proteins as informed by homology-based modeling (see Figure 4C). We also substituted Bpa for N171 (a catalytic residue in the phospho-transfer active site) and Y209 (the autophosphorylation phospho-acceptor in the activation loop) as negative controls for the pY209 immunoassay. Although Bpa substituted at some positions in Smk1 decreased the recovery of the Ssp2^{KAD}-GST/Smk1 complex (e.g., Y145 in Figure 4), most of the mutants had little effect on recovery. Other than the N171 and Y209 Bpa substitution mutants that obliterated pY209 immunoreactivity, only a single mutant was identified that substantially decreased the autophosphorylation activity of the complex (L368). Many of the Bpa substitution sites were selected in part because they are predicted to be solvent-exposed and outside of the ATP-binding pocket and phospho-transfer active site. Nevertheless, these results may suggest that the interaction of Smk1 and Ssp2 and the consequent transfer of phosphate from ATP to the Y209 phosphoacceptor are relatively tolerant to Bpa substitution. Significantly, of the six Smk1 Bpa substitution mutants tested, only the Y38 substitution substantially increased the abundance of a high-molecular weight Smk1 immunoreactive complex (Figure 4A). This high-molecular weight complex was immunoreactive with the pY209 antiserum and with a GST antiserum (Figure 4B). Y38 is an evolutionary conserved residue found in most MAPKs that is amino-terminal to the G-rich ATP-binding residues in subdomain I of the kinase. On the basis of the three-dimensional structures of other MAPKs, Y38 is predicted to be at the end of a β-sheet adjacent to the ATP-binding pocket of Smk1 (Figure 4C). These observations suggest that Ssp2^{KAD} can bind and activate the Smk1-Y38Bpa mutant protein and that the Bpa-substituted residue in this complex is within 4 Å of a cross-linkable atom in Ssp2. The proximity of Y38 to the predicted ATP-binding pocket of Smk1 raises the possibility that Ssp2 influences Smkl's interaction with ATP.

Residues in KARL1 and KARL2 Can Be Cross-Linked to Smk1.

We next tested whether Ssp2^{KAD}-GST containing Bpa substitutions at various positions can be cross-linked to Smk1. For these experiments, we selected substitution positions within KARL1 and KARL2 that are predicted to be surface-exposed on the basis of the sequence similarity to canonical RRMs that were informed by structural predictions (see Figure 1). We also tested several substitution positions at or near the F residues in KARL1 and KARL2 that are required for function. These data are presented in Figure 5. The Bpa substitution mutants in Ssp2^{KAD} fell into four classes based upon formation of UV-inducible cross-links with Smk1, immunological properties, and the influence of the Bpa substitution on autophosphorylation. Class 1 mutants showed high levels of UV-dependent high-molecular weight species that were immunoreactive with both the Smk1 and the pY209 antisera. One of these class 1 mutants is at position Y223 in KARL1, two residues carboxy-terminal to F211, which mutational analyses indicate is important for Ssp2's ability to activate Smk1 (Figure 5A). These data suggest that Y223 in Ssp2 is located within 4 Å of Smk1 in the active Smk1/Ssp2 complex but that the Y223 side chain is not required for formation of a

functional complex. A second class 1 mutant is at position V317 in KARL2, midway between residues F307 and F327 that mutational data suggest are important for the Ssp2/Smk1 interaction. The class 1 data indicate that both KARLs directly contact Smk1. Class 2 mutants showed high levels of a UV-dependent high-molecular weight complex that was immunoreactive with the Smk1 antisera but not with the pY209 antisera. A single class 2 mutant was identified, and this mutant is at F307. These data provide biochemical evidence that F307 is in close contact with Smk1 in the Ssp2/Smk1 complex and that the F307 side chain is essential for Ssp2's ability to activate Smk1. This interpretation is consistent with the inability of Ssp2-F307A to activate Smk1 (Figure 1). Class 3 mutants eliminated activation of Smk1 as measured using the pY209 antiserum and generated near background levels of cross-links with Smk1 (R185 and F211 in KARL1 and F327 and I330 in KARL2). These mutations could eliminate the ability of Ssp2 to activate Smk1 by perturbing the folding of the KARLs or by altering side chains that directly interact with Smk1. Class 4 mutants retained the ability to activate Smk1 autophosphorylation and formed only background levels of UV-dependent cross-links with Smk1 (e.g., Y195 and F229 in KARL1 and S324 in KARL2). These amino acids are not required for Ssp2 to bind and activate the MAPK It should be pointed out that because the structures of Smk1 and the Smk1/Ssp2 complex are not currently known, we cannot rule out the possibility that Bpa at various positions in Ssp2 influences an inactive to active equilibrium and therefore crosslinking. Despite this caveat, the cross-linking data indicate that both KARLs interact with Smk1 and that at least one of the KARLs interacts near residue Y38.

DISCUSSION

Previous studies demonstrated that Ssp2 is a modular protein consisting of an amino-terminal targeting domain that localizes the protein to specific intracellular membranes (PSMs) and a carboxy-terminal kinase activating domain that binds Smk1 and activates the enzyme.[24,25] While the kinase-activating domain promotes the intramolecular autophosphorylation of Smk1 on its activation-loop tyrosine (Y209), thereby increasing catalytic output of the enzyme, it is capable of activating catalytic output of a Smk1-Y209F phospho-site mutant (albeit to a extent lower than that of wild-type kinase). These observations suggest that Ssp2 activates Smk1 first by inducing structural rearrangements to the MAPK that must occur before activation-loop autophosphorylation takes place. These rearrangements could influence the affinity for ATP, the orientation of bound ATP, or other properties of the kinase associated with the activated state that in turn permit transfer of phosphate to Y209. Understanding how Ssp2 unlocks Smk1 to permit activating autophosphorylation to occur is therefore important for understanding the Ssp2 activation mechanism. In this study, we have shown that the activation of Smk1 by Ssp2 requires two separable functional motifs that are related to RRMs: an 84-residue KARL1 segment (amino acids 162–245) and a 106-residue KARL2 segment (amino acids 266–371).

Two MAPKs that undergo regulated activation-loop autophosphorylation have previously been studied using structural methods. The first is the mammalian p38-α MAPK that is activated to *cis* autophosphorylate both the T and Y residues in its activation loop by the TAB1-binding protein following myocardial ischemia and other stresses.[48] A 45-residue peptide from TAB1 is sufficient to activate p38-α, and this peptide binds two surfaces on the

C-lobe of the kinase. This bipartite interaction triggers allosteric rearrangements to p38-α that increase the affinity of the N-lobe for ATP and also trigger changes to the activation-loop segment. The second structural study of regulated MAPK autophosphorylation was performed on the Fus3 MAPK from yeast.[6] While Fus3 is canonically activated in response to mating pheromones, the Ste5 scaffold also induces Fus3 to autophosphorylate its activation-loop Y in *cis* after the initial phase of mating pheromone/receptor stimulation has occurred. This interaction causes Fus3 to phosphorylate residues in Ste5 that downregulate signaling in a negative feedback loop. A 28-residue peptide of Ste5 is sufficient to activate Fus3 autophosphorylation in vitro, and this peptide binds to the N- and C-lobes of the kinase. One conclusion from the Ssp2/Smk1 cross-linking analyses is that residues in both KARL1 and KARL2 interact with Smk1. These data indicate that Ssp2 binds Smk1 through a bipartite mechanism, yet the Ssp2 mechanism is different from those of both TAB1 and Ste5 by utilizing folded protein motifs to engage the MAPK instead of short peptide sequences. In the case of Fus3, a flexible linker separates the peptide motifs in Ste5 that bind Fus3 and the length of the linker is important for activation. It has been proposed that the peptide triggers autophosphorylation by promoting a shift in the relative orientation of the N- and C-domains of the kinase. Our data demonstrate that the two KARLs can activate Smk1 when expressed as separate proteins in bacterial cells. These findings suggest that Ssp2 does not require a fixed-length linker strategy to activate Smk1 as has been proposed for Ste5/Fus3. Unlocking the kinase for catalysis by increasing the affinity of the enzyme for ATP is a potential step in the activation of Smk1. Consistent with this idea, our cross-linking studies indicate that at least one of the KARLs in Ssp2 can be cross-linked to Y38 in Smk1, a conserved MAPK residue located near β-sheets predicted to be adjacent to the ATP-binding pocket. Interestingly, this region of Smk1 corresponds to the region of Fus3 that is bound by one of the two interacting motifs in the Ste5 peptide (indicated by red shading in the kinase model in Figure 4C). Our analyses identified only a single Smk1 Bpa substitution allele that strongly increased the level of cross-linking to Ssp2, and we therefore do not know whether the second hypothesized region of Smk1 that binds to Ssp2 is in the N-lobe or in the C-lobe. Although sequence comparisons place Smk1 firmly in the MAPK family of protein kinases, it appears to be regulated by several mechanisms that control the related CDK family of kinases. Thus, Smk1 is controlled by a CDK-activating kinase (Cak1) and an activating protein that binds the kinase at a specific stage of the cell cycle. Nevertheless, a segment comparable to the Y38 segment of Smk is not found in CDKs, and most cyclins bind on the opposite side of the catalytic core to where Y38 is predicted to reside.[49] These findings suggest that the cyclin/CDK and Ssp2/Smk1 interactions are unrelated. Defining the topology of the Ssp2/Smk1 complex and the rearrangements in Smk1 that occur upon Ssp2 binding will require further studies.

RRMs are ancient motifs, and numerous RRM variants are encoded in eukaryotic genomes. Examples of RRM-like motifs that bind protein have been described previously.[50,51] However, the RRM-like motif/protein interactions that have been described thus far involve RRMs that are directly connected to RNA-mediated processes such as translational initiation, RNA splicing, and responses to viral RNAs, and some of these RRMs bind both RNA and protein. These observations suggest that many protein-binding RRMs evolved from RNA-binding RRMs via paths that linked shared processes. While it remains possible

that there is an undiscovered role for RNA in the Smk1 pathway, we are at present unable to directly connect Ssp2 to RNA-mediated processes in the cell. Whether Smk1/Ssp2 is regulated by RNAs or regulates specific RNAs will require further investigation.

Protein kinase R (PKR) and GCN2 are kinases that phosphorylate the α-subunit of initiation factor 2 (eIF2α) to inhibit translation.[52] Both of these kinases contain RRMs in their protein coding sequence that trigger catalytic output when bound by viral RNAs (PKR) or uncharged tRNAs (GCN2). The binding of RNA to the RRMs in PKR and GCN2 promotes dimerization and *trans* autophosphorylation of activation-loop T residues, while Ssp2 binding unlocks the kinase and triggers the *cis* autophosphorylation of the activation-loop Y. Thus, although the PKR, GCN2, and Smk1 kinases are all regulated by related motifs, the mechanism of Smk1 activation by Ssp2 is distinct. Are RRM-like motifs used to activate other protein kinases via a similar mechanism? Bioinformatic analyses reveal close relatives of Ssp2 and Smk1 in *Ascomycetes,* and Ssp2 and Smk1 relatives can be identified in the fungal lineage connecting *Saccharomyces* to *Candida.* We have thus far been unable to identify a Smk1/Ssp2 pair in higher organisms. However, these analyses are complicated by the numerous kinases and RRMs encoded by eukaryotic genomes. For now, the existence of a Ssp2/Smk1-like mechanism in animal cells remains an open question.

Acknowledgments

Funding

This research was supported by National Institutes of Health Grant 5R01GM120090 (to E.W.).

ABBREVIATIONS

MAPK	mitogen-activated protein kinase
RRM	RNA recognition motif
KARL	kinase-activating RRM-like
KAD	kinase-activating domain
TD	targeting domain
SDS	sodium dodecyl sulfate
PMSF	phenylmethanesulfonyl fluoride
Bpa	*p*-benzoyl-L-phenylalanine
MBP	maltose-binding protein
GST	glutathione *S*-transferase

REFERENCES

(1). Chen RE, and Thorner J (2007) Function and regulation in MAPK signaling pathways: lessons learned from the yeast *Saccharomyces cerevisiae*. Biochim. Biophys. Acta, Mol. Cell Res 1773, 1311–1340.

(2). Coulombe P, and Meloche S (2007) Atypical mitogen-activated protein kinases: structure, regulation and functions. Biochim. Biophys. Acta, Mol. Cell Res 1773, 1376–1387.

(3). Pimienta G, and Pascual J (2007) Canonical and alternative MAPK signaling. Cell Cycle 6, 2628–2632. [PubMed: 17957138]

(4). Salvador JM, Mittelstadt PR, Guszczynski T, Copeland TD, Yamaguchi H, Appella E, Fornace AJ Jr., and Ashwell JD (2005) Alternative p38 activation pathway mediated by T cell receptor-proximal tyrosine kinases. Nat. Immunol 6, 390–395. [PubMed: 15735648]

(5). Ge B, Gram H, Di Padova F, Huang B, New L, Ulevitch RJ, Luo Y, and Han J (2002) MAPKK-independent activation of p38alpha mediated by TAB1-dependent autophosphorylation of p38alpha. Science 295, 1291–1294. [PubMed: 11847341]

(6). Bhattacharyya RP, Remenyi A, Good MC, Bashor CJ, Falick AM, and Lim WA (2006) The Ste5 scaffold allosterically modulates signaling output of the yeast mating pathway. Science 311, 822–826. [PubMed: 16424299]

(7). Coyle SM, Flores J, and Lim WA (2013) Exploitation of latent allostery enables the evolution of new modes of MAP kinase regulation. Cell 154, 875–887. [PubMed: 23953117]

(8). Rossomando AJ, Wu J, Michel H, Shabanowitz J, Hunt DF, Weber MJ, and Sturgill TW (1992) Identification of Tyr-185 as the site of tyrosine autophosphorylation of recombinant mitogen-activated protein kinase p42mapk. Proc. Natl. Acad. Sci. U. S. A 89, 5779–5783. [PubMed: 1378617]

(9). Crews CM, Alessandrini AA, and Erikson RL (1991) Mouse Erk-1 gene product is a serine/threonine protein kinase that has the potential to phosphorylate tyrosine. Proc. Natl. Acad. Sci. U. S. A 88, 8845–8849. [PubMed: 1717989]

(10). Seger R, Ahn NG, Boulton TG, Yancopoulos GD, Panayotatos N, Radziejewska E, Ericsson L, Bratlien RL, Cobb MH, and Krebs EG (1991) Microtubule-associated protein 2 kinases, ERK1 and ERK2, undergo autophosphorylation on both tyrosine and threonine residues: implications for their mechanism of activation. Proc. Natl. Acad. Sci. U. S. A 88, 6142–6146. [PubMed: 1712480]

(11). Wu J, Rossomando AJ, Her JH, Del Vecchio R, Weber MJ, and Sturgill TW (1991) Autophosphorylation in vitro of recombinant 42-kilodalton mitogen-activated protein kinase on tyrosine. Proc. Natl. Acad. Sci. U. S. A 88, 9508–9512. [PubMed: 1835084]

(12). Han J, Miranda-Saavedra D, Luebbering N, Singh A, Sibbet G, Ferguson MA, and Cleghon V (2012) Deep evolutionary conservation of an intramolecular protein kinase activation mechanism. PLoS One 7, No. e29702.

(13). Kinstrie R, Luebbering N, Miranda-Saavedra D, Sibbet G, Han J, Lochhead PA, and Cleghon V (2010) Characterization of a domain that transiently converts class 2 DYRKs into intramolecular tyrosine kinases. Sci. Signaling 3, ra16.

(14). Lochhead PA, Kinstrie R, Sibbet G, Rawjee T, Morrice N, and Cleghon V (2006) A chaperone-dependent GSK3beta transitional intermediate mediates activation-loop autophosphorylation. Mol. Cell 24, 627–633. [PubMed: 17188038]

(15). Lochhead PA, Sibbet G, Kinstrie R, Cleghon T, Rylatt M, Morrison DK, and Cleghon V (2003) dDYRK2: a novel dualspecificity tyrosine-phosphorylation-regulated kinase in Drosophila. Biochem. J 374, 381–391. [PubMed: 12786602]

(16). Lochhead PA, Sibbet G, Morrice N, and Cleghon V (2005) Activation-loop autophosphorylation is mediated by a novel transitional intermediate form of DYRKs. Cell 121, 925–936. [PubMed: 15960979]

(17). Fu Z, Schroeder MJ, Shabanowitz J, Kaldis P, Togawa K, Rustgi AK, Hunt DF, and Sturgill TW (2005) Activation of a nuclear Cdc2-related kinase within a mitogen-activated protein kinase-like TDY motif by autophosphorylation and cyclin-dependent protein kinase-activating kinase. Mol. Cell. Biol 25, 6047–6064. [PubMed: 15988018]

(18). Abe MK, Kahle KT, Saelzler MP, Orth K, Dixon JE, and Rosner MR (2001) ERK7 is an autoactivated member of the MAPK family. J. Biol. Chem 276, 21272–21279. [PubMed: 11287416]

(19). Schindler K, Benjamin KR, Martin A, Boglioli A, Herskowitz I, and Winter E (2003) The Cdk-activating kinase Cak1p promotes meiotic S phase through Ime2p. Mol. Cell. Biol 23, 8718–8728. [PubMed: 14612412]

(20). Schindler K, and Winter E (2006) Phosphorylation of Ime2 regulates meiotic progression in *Saccharomyces cerevisiae*. J. Biol. Chem 281, 18307–18316. [PubMed: 16684773]

(21). Krisak L, Strich R, Winters RS, Hall JP, Mallory MJ, Kreitzer D, Tuan RS, and Winter E (1994) *SMK1,* a developmentally regulated MAP kinase, is required for spore wall assembly in *Saccharomyces cerevisiae*. Genes Dev 8, 2151–2161. [PubMed: 7958885]

(22). McDonald CM, Cooper KF, and Winter E (2005) The Ama1-directed anaphase-promoting complex regulates the Smk1 mitogen-activated protein kinase during meiosis in yeast. Genetics 171, 901–911. [PubMed: 16079231]

(23). McDonald CM, Wagner M, Dunham MJ, Shin ME, Ahmed NT, and Winter E (2008) The Ras/cAMP pathway and the CDK-like kinase Ime2 regulate the MAPK Smk1 and spore morphogenesis in *Saccharomyces cerevisiae*. Genetics 181, 511–523. [PubMed: 19087957]

(24). Tio CW, Omerza G, Phillips T, Lou HJ, Turk BE, and Winter E (2017) Ssp2 Binding Activates the Smk1 Mitogen-Activated Protein Kinase. Mol. Cell. Biol 37, 607–616.

(25). Tio CW, Omerza G, Sunder S, and Winter E (2015) Autophosphorylation of the Smk1 MAPK is spatially and temporally regulated by Ssp2 during meiotic development in yeast. Mol. Biol. Cell 26, 3546–3555. [PubMed: 26246597]

(26). Wagner M, Briza P, Pierce M, and Winter E (1999) Distinct steps in yeast spore morphogenesis require distinct Smk1 MAP kinase thresholds. Genetics 151, 1327–1340. [PubMed: 10101160]

(27). Wagner M, Pierce M, and Winter E (1997) The CDK-activating kinase Cak1 can dosage suppress sporulation defects of Smk1 MAP kinase mutants and is required for spore wall morphogenesis in *Saccharomyces cerevisiae*. EMBO J 16, 1305–1317. [PubMed: 9135146]

(28). Whinston E, Omerza G, Singh A, Tio CW, and Winter E (2013) Activation of the Smk1 mitogen-activated protein kinase by developmentally regulated autophosphorylation. Mol. Cell. Biol 33, 688–700. [PubMed: 23207907]

(29). Pierce M, Benjamin KR, Montano SP, Georgiadis MM, Winter E, and Vershon AK (2003) Sum1 and Ndt80 proteins compete for binding to middle sporulation element sequences that control meiotic gene expression. Mol. Cell. Biol 23, 4814–4825. [PubMed: 12832469]

(30). Pierce M, Wagner M, Xie J, Gailus-Durner V, Six J, Vershon AK, and Winter E (1998) Transcriptional regulation of the *SMK1* mitogen-activated protein kinase gene during meiotic development in *Saccharomyces cerevisiae*. Mol. Cell. Biol 18, 5970–5980. [PubMed: 9742114]

(31). Neiman AM (1998) Prospore membrane formation defines a developmentally regulated branch of the secretory pathway in yeast. J. Cell Biol 140, 29–37. [PubMed: 9425151]

(32). Neiman AM (2005) Ascospore formation in the yeast *Saccharomyces cerevisiae*. Microbiol. Mol. Biol. Rev 69, 565–584. [PubMed: 16339736]

(33). Neiman AM (2011) Sporulation in the budding yeast *Saccharomyces cerevisiae*. Genetics 189, 737–765. [PubMed: 22084423]

(34). Omerza G, Tio CW, Philips T, Diamond A, Neiman AM, and Winter E (2018) The meiosis-specific Cdc20 family-member Ama1 promotes binding of the Ssp2 activator to the Smk1 MAP kinase. Mol. Biol. Cell 29, 66–74. [PubMed: 29118076]

(35). Sarkar PK, Florczyk MA, McDonough KA, and Nag DK (2002) *SSP2* a sporulation-specific gene necessary for outer spore wall assembly in the yeast *Saccharomyces cerevisiae*. Mol. Genet. Genomics 267, 348–358. [PubMed: 12073037]

(36). Berchowitz LE, Gajadhar AS, van Werven FJ, De Rosa AA, Samoylova ML, Brar GA, Xu Y, Xiao C, Futcher B, Weissman JS, White FM, and Amon A (2013) A developmentally regulated translational control pathway establishes the meiotic chromosome segregation pattern. Genes Dev 27, 2147–2163. [PubMed: 24115771]

(37). Berchowitz LE, Kabachinski G, Walker MR, Carlile TM, Gilbert WV, Schwartz TU, and Amon A (2015) Regulated Formation of an Amyloid-like Translational Repressor Governs Gametogenesis. Cell 163, 406–418 [PubMed: 26411291]

(38). Carpenter K, Bell RB, Yunus J, Amon A, and Berchowitz EL (2018) Phosphorylation-Mediated Clearance of Amyloid-like Assemblies in Meiosis. Dev. Cell 45, 392–405e396. [PubMed: 29738715]

(39). Jin L, Zhang K, Sternglanz R, and Neiman AM (2017) Predicted RNA Binding Proteins Pes4 and Mip6 Regulate mRNA Levels, Translation, and Localization during Sporulation in Budding Yeast. Mol. Cell. Biol 37, 408–416.

(40). Longtine MS, McKenzie A III, Demarini DJ, Shah NG, Wach A, Brachat A, Philippsen P, and Pringle JR (1998) Additional modules for versatile and economical PCR-based gene deletion and modification in *Saccharomyces cerevisiae*. Yeast 14, 953–961. [PubMed: 9717241]

(41). Ryu Y, and Schultz PG (2006) Efficient incorporation of unnatural amino acids into proteins in Escherichia coli. Nat. Methods 3, 263–265. [PubMed: 16554830]

(42). Corbi D, Sunder S, Weinreich M, Skokotas A, Johnson ES, and Winter E (2014) Multisite phosphorylation of the Sum1 transcriptional repressor by S-phase kinases controls exit from meiotic prophase in yeast. Mol. Cell. Biol 34, 2249–2263. [PubMed: 24710277]

(43). Waterhouse A, Bertoni M, Bienert S, Studer G, Tauriello G, Gumienny R, Heer FT, de Beer TAP, Rempfer C, Bordoli L, Lepore R, and Schwede T (2018) SWISS-MODEL: homology modelling of protein structures and complexes. Nucleic Acids Res 46, W296–W303. [PubMed: 29788355]

(44). Emsley P, and Cowtan K (2004) Coot: model-building tools for molecular graphics. Acta Crystallogr., Sect. D: Biol. Crystallogr 60, 2126–2132. [PubMed: 15572765]

(45). Jones DT (1999) Protein secondary structure prediction based on position-specific scoring matrices. J. Mol. Biol 292, 195–202. [PubMed: 10493868]

(46). Daubner GM, Clery A, and Allain FH (2013) RRM-RNA recognition: NMR or crystallography⋯and new findings. Curr. Opin. Struct. Biol 23, 100–108. [PubMed: 23253355]

(47). Young TS, Ahmad I, Yin JA, and Schultz PG (2010) An enhanced system for unnatural amino acid mutagenesis in *E. coli*. J. Mol. Biol 395, 361–374. [PubMed: 19852970]

(48). DeNicola GF, Martin ED, Chaikuad A, Bassi R, Clark J, Martino L, Verma S, Sicard P, Tata R, Atkinson RA, Knapp S, Conte MR, and Marber MS (2013) Mechanism and consequence of the autoactivation of p38alpha mitogen-activated protein kinase promoted by TAB1. Nat. Struct. Mol. Biol 20, 1182–1190. [PubMed: 24037507]

(49). Wood DJ, and Endicott JA (2018) Structural insights into the functional diversity of the CDK-cyclin family. Open Biol 8, 180112. [PubMed: 30185601]

(50). Clery A, Blatter M, and Allain FH (2008) RNA recognition motifs: boring? Not quite. Curr. Opin. Struct. Biol 18, 290–298. [PubMed: 18515081]

(51). Loerch S, and Kielkopf CL (2016) Unmasking the U2AF homology motif family: a bona fide protein-protein interaction motif in disguise. RNA 22, 1795–1807. [PubMed: 27852923]

(52). Donnelly N, Gorman AM, Gupta S, and Samali A (2013) The eIF2alpha kinases: their structures and functions. Cell. Mol. Life Sci 70, 3493–3511. [PubMed: 23354059]

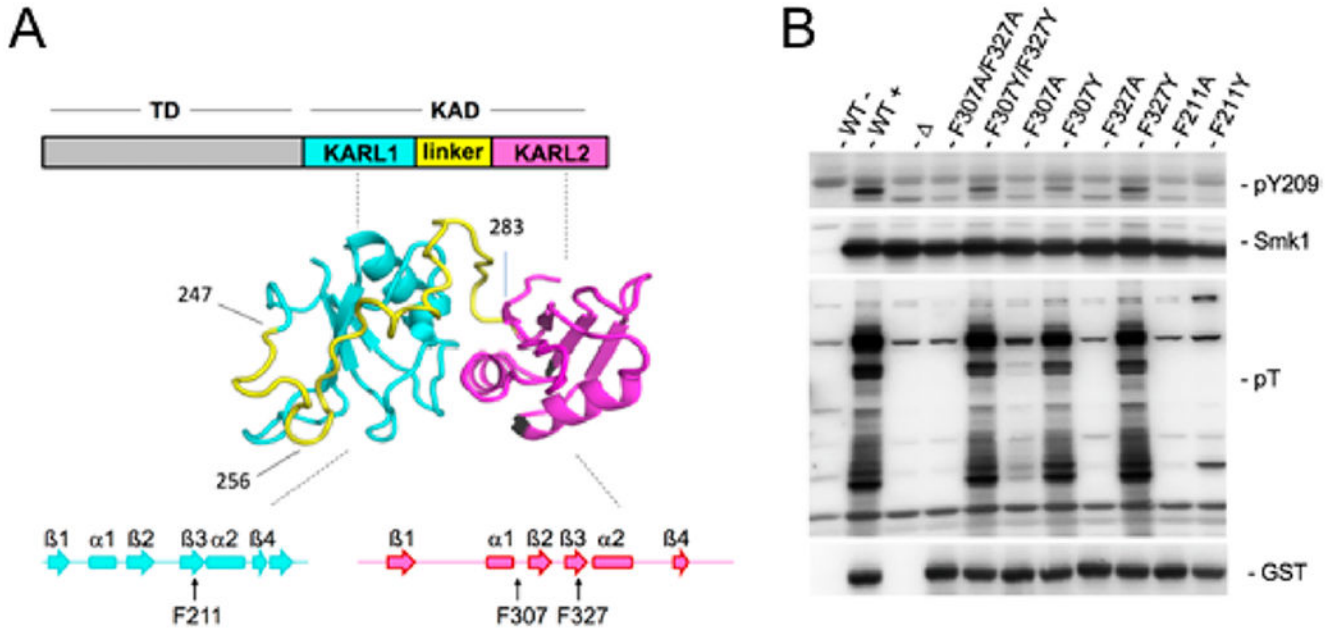

Figure 1.

(A) Diagram of Ssp2 showing the TD and the KAD (top). The KAD is further subdivided into KARL1 (turquoise), the linker (yellow), and KARL2 (magenta). The KAD modeled after the structure of the polypyrimidine tract-binding protein (middle) and a secondary structure model of the KAD predicted by PSIPRED (below) are shown with Ssp2 residue numbers in the linker indicated. The positions of F211 and F327, corresponding to the F residues in canonical RRMs that stack with RNA bases, and F307, a residue that is present in a subset of RRMs, are indicated with upward arrows. (B) Mutational analyses of F211, F307, and F327 in Ssp2. Bacteria were transformed with plasmids that direct the expression of Smk1 and either wild-type or mutant forms of $Ssp2^{KAD}$-GST as indicated. The most leftward lane shows bacterial cells analyzed in the absence of an inducer (–) as a control. Transformants were induced and total cellular extracts analyzed by immunoblots using the indicated antibodies. The lanes correspond to the following plasmids: WT, pJT118; Δ, pJT114; F307A/F327A, pAR10; F307Y/F327Y, pAR11; F307A, pAR4; F307Y, pAR6; F327A, pAR7; F327Y, pAR9; F211A, pAR1; F211Y, pAR3 (Table 2).

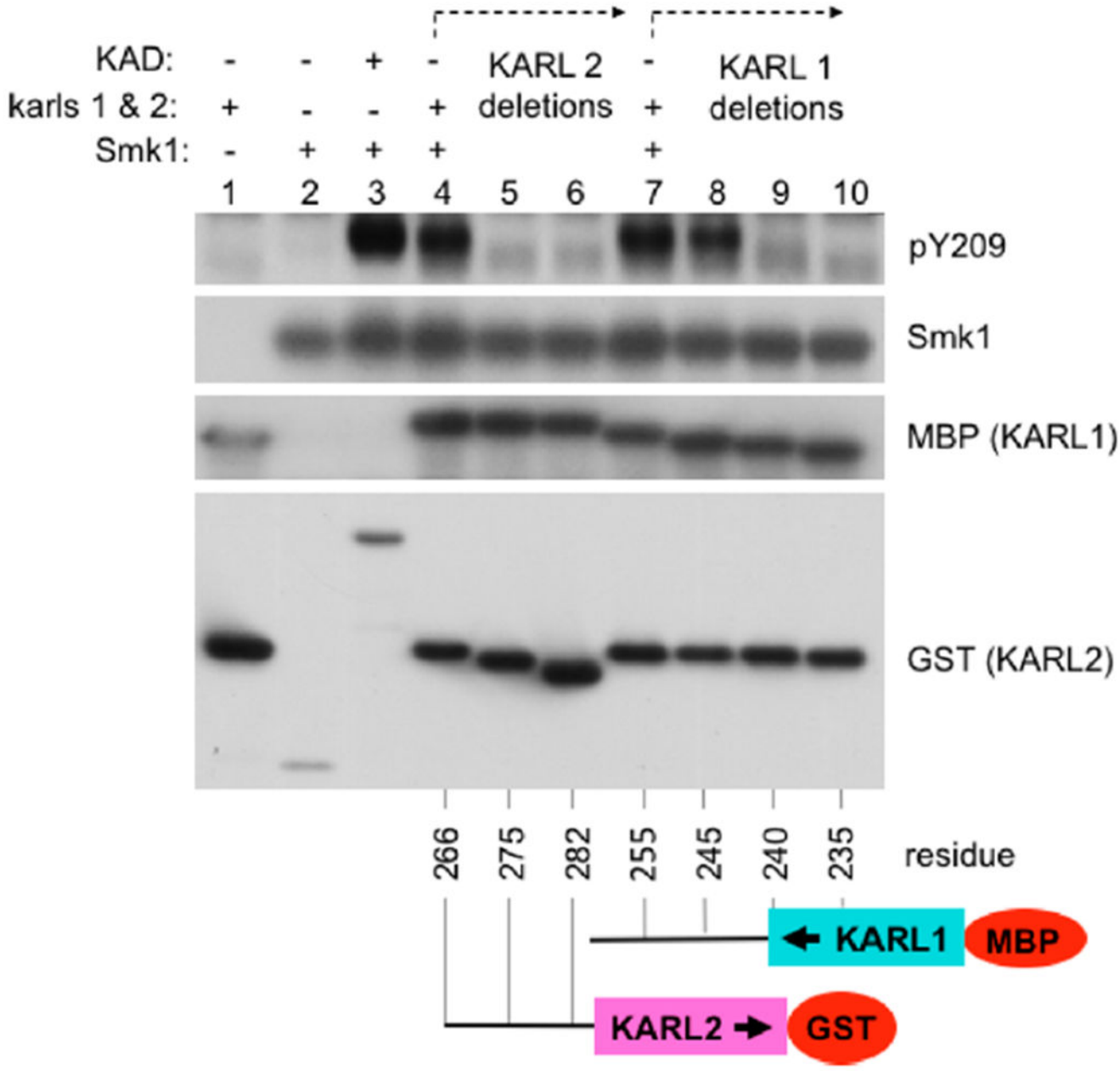

Figure 2.

KARL1 and KARL2 are functional when expressed as separate proteins. Bacteria producing residues 162–265 of Ssp2 fused to the C-terminus of MBP (KARL1), residues 266–371 of Ssp2 fused to the N-terminus of GST (KARL2), $Ssp2^{KAD}$-GST (KAD), and Smk1, as indicated above, were assayed by immunoblotting using the antisera against the proteins indicated on the right. The KARL2 deletion mutants diagrammed below (vertical lines indicating deletion end points) were co-expressed with the functional MBP-$Ssp2^{162–265}$ KARL1 protein, and the KARL1 deletions diagrammed below were co-expressed with the functional $Ssp2^{266–371}$-GST (KARL2) protein. The lanes correspond to the following plasmids: lane 1, pTP39 and pTP36; lane 2, pJT114 and pACYDuet-1 (empty vector); lane

3, pJT118 and pACYDuet-1; lane 4, pTP35 and pTP14; lane 5, pTP35 and pTP41; lane 6, pTP35 and pTP15; lane 7, pTP39 and pTP14; lane 8, pTP40 and pTP14; lane 9, pTP44 and pTP14; lane 10, pTP45 and pTP14 (Table 2).

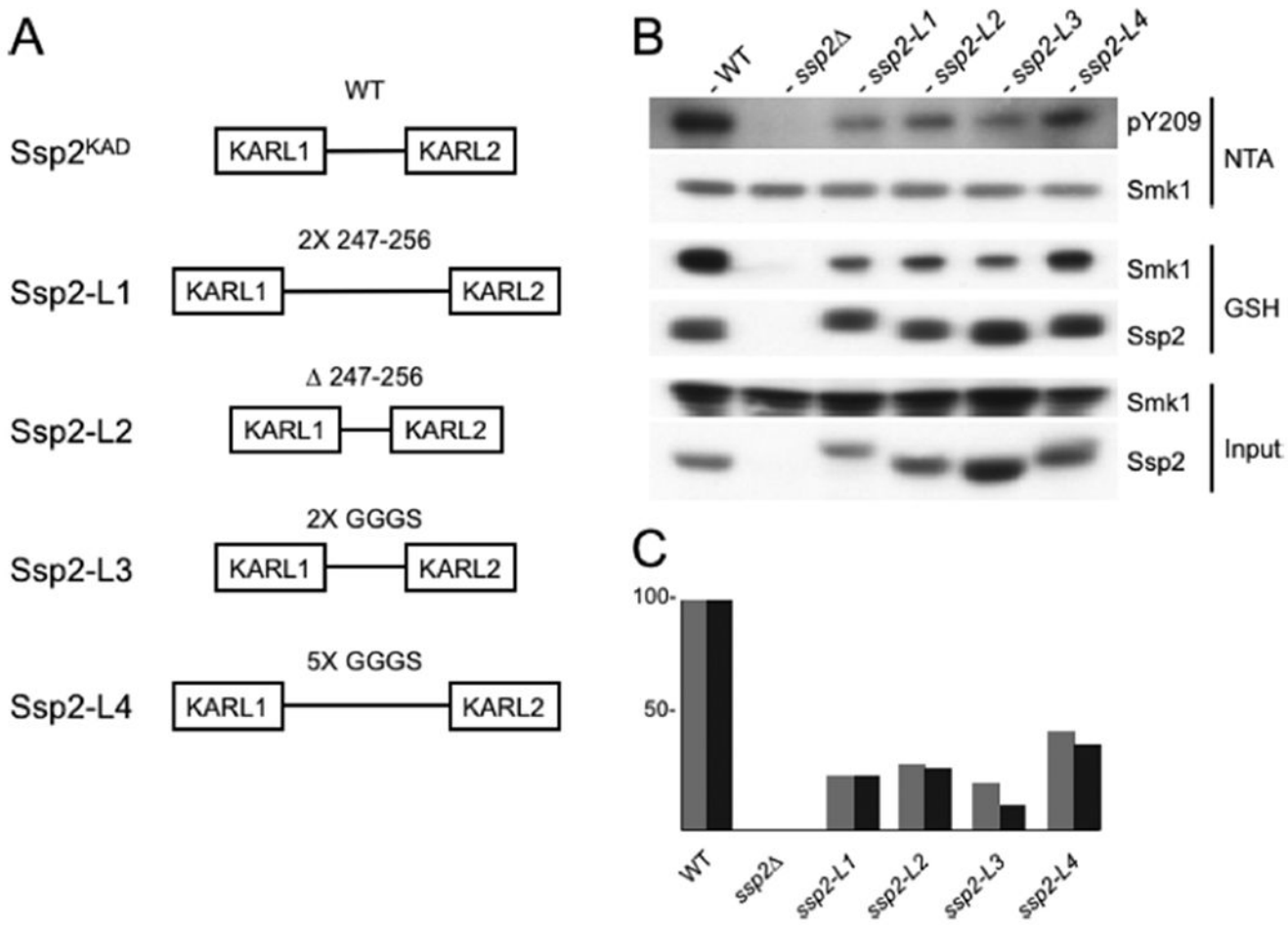

Figure 3.

The *SSP2* linker can tolerate substantial mutation. (A) Diagram of linker mutants L1–L4 in Ssp2. (B) Diploid *SMK1-HH/SMK1-HH* yeast containing one chromosomal copy of the indicated *SSP2*^{KAD}*-GST* linker derivatives were transferred to sporulation medium, and cells were collected 8.5 h post-induction (when >75% of cells had completed MII). Smk1-HH was purified using nickel beads (NTA), and the fraction of Smk1-HH that had autophosphorylated Y209 was scored using pY209 and HA (Smk1) antibodies as indicated. The Ssp2-GST derivatives were purified from a portion of the extracts using glutathione agarose (GSH), and the relative fraction of Smk1 that was bound to Ssp2 was scored using antibodies against HA (Smk1) and GST (Ssp2). The input serves as a control for the amount of Smk1 and Ssp2 in the extracts. (C) The fraction of cells that completed the sporulation program was scored by counting asci that contained two or more refractile spores (dark bars) and are plotted with the fraction of Smk1 that had autophosphorylated Y209 (relative pY209:Smk1 ratios with the wild-type *SSP2*^{KAD}*-GST* strain taken to be 1.0) (lighter gray bars). The following yeast strains were used in these experiments: JTY88 (WT), TPY13 (*ssp2*Δ), TPY29 (*ssp2-L1*), TPY28 (*ssp2-L2*), TPY30 (*ssp2-L3*), and TPY36 (*ssp2-L4*) (Table 1).

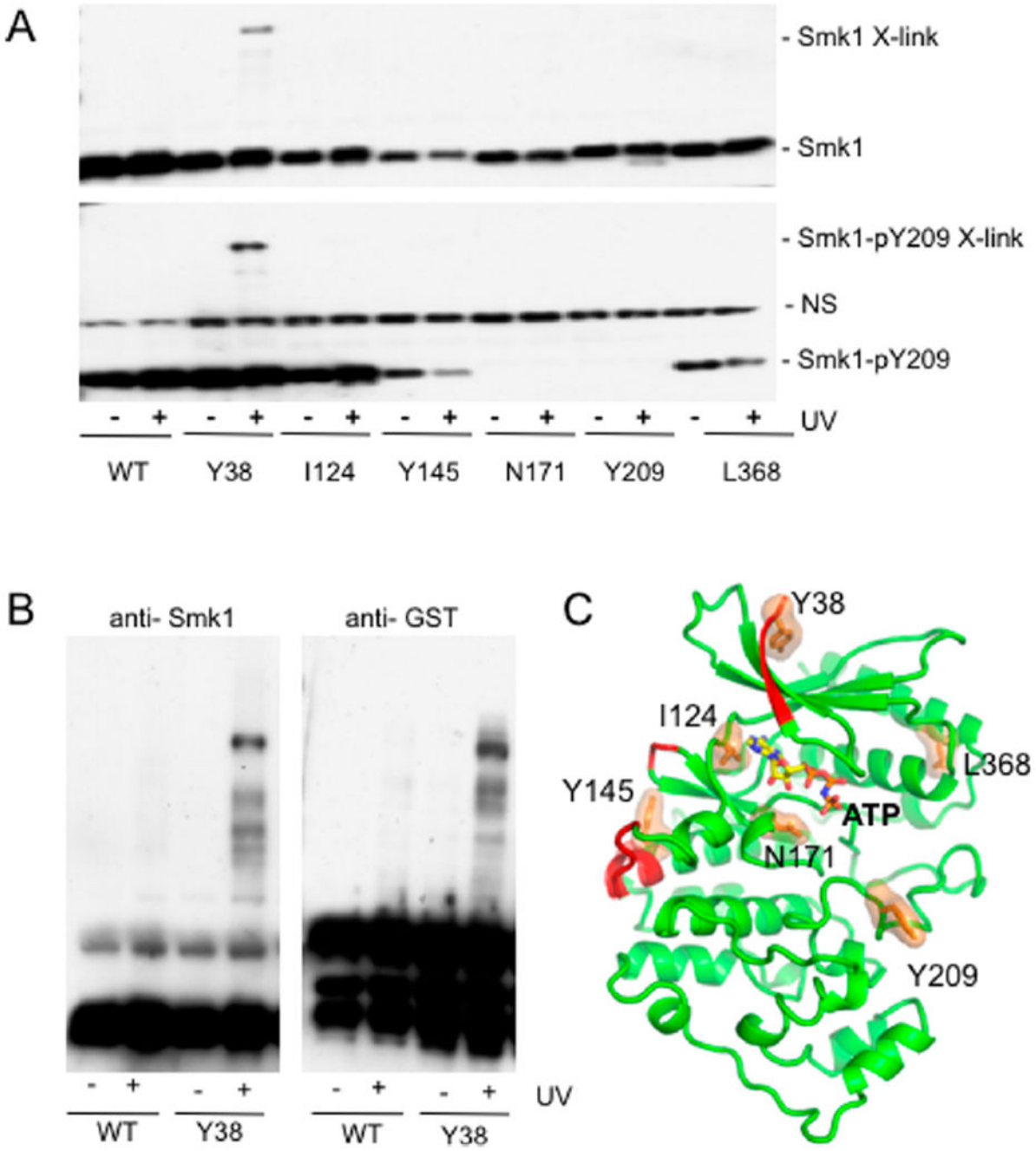

Figure 4.

Residue near the ATP-binding pocket of Smk1 that is within 4 Å of Ssp2. (A) Smk1 derivatives containing the cross-linkable amino acid, Bpa, at the indicated positions were co-expressed in bacteria with $Ssp2^{KAD}$-GST. Complexes were purified using reduced glutathione, and one half of the preparation was irradiated with UV light (+) and the other half was untreated (−). Samples were analyzed by electrophoresis through denaturing electrophoretic gels and immunoblotting using a Smk1 antibody (top) or a pY209 antiserum (bottom). The cross-linked (X-link) species migrates at approximately 130 kDa, a molecular

weight slightly larger than the predicted molecular weight of a Smk1/Ssp2^{KAD}-GST complex. NS (nonspecific) indicates a bacterial protein that cross-reacts with the pY209 antiserum. (B) Samples were processed as described for panel A and assayed using a GST or a Smk1 antiserum as indicated. All of the bacterial strains in these experiments contained pEVOL (provides the tRNA/synthetase pair that permits incorporation of Bpa at amber suppressible codons) and pJT115 (WT) or the derivatives of pJT115-containing amber codons at the indicated positions as listed in Table 2. (C) Smk1 modeled after ERK5. Positions substituted with Bpa and analyzed in panels A and B are indicated (tan). Residues of Smk1 that correspond to residues in Fus3 that interact with a peptide from Ste5 that triggers autophosphorylation of Fus3's activation-loop Y are colored red (see Discussion).

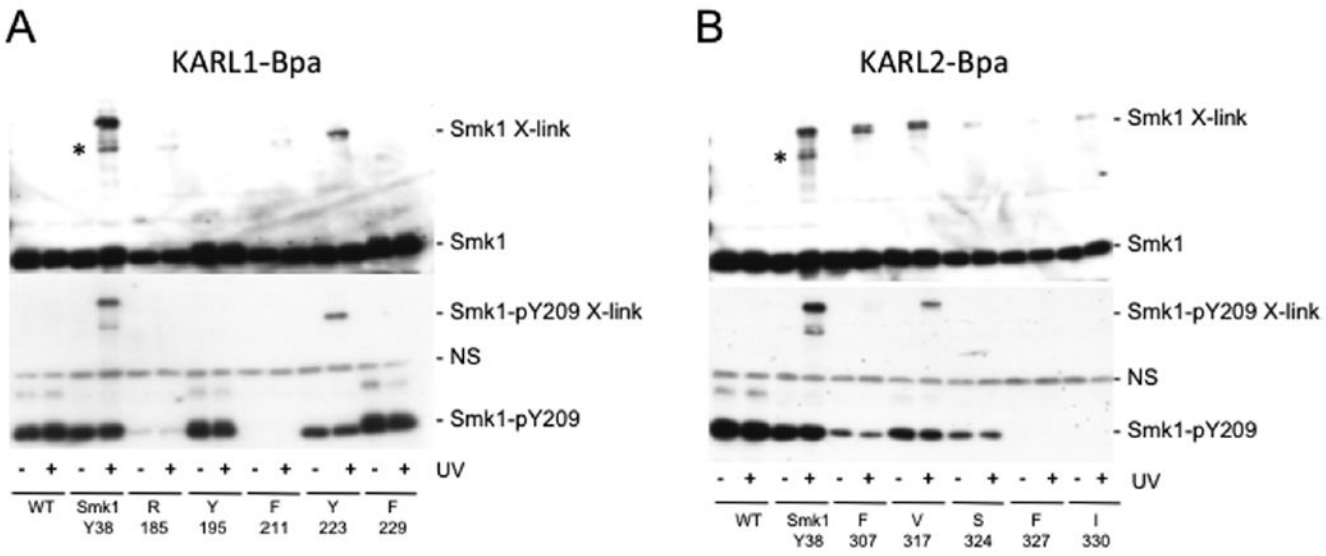

Figure 5.

Residues in both KARL1 and KARL2 are within 4 Å of Smk1. Ssp2^{KAD}-GST derivatives containing Bpa at the indicated positions in (A) KARL1 or (B) KARL2 were co-expressed with Smk1 in bacteria. Complexes were purified using reduced glutathione beads and exposed to UV light (+) or left untreated (−). Samples were then analyzed by denaturing electrophoresis and immunobloting using Smk1 and Smk1-Y209p antisera. All of the bacterial strains in these experiments contained pEVOL (provides the tRNA/synthetase pair that permits incorporation of Bpa at amber suppressible codons) and pJT115 (WT) or the derivatives of pJT115-containing amber codons at the indicated positions as listed in Table 2. The Smk1 Y38 samples, which contain Bpa at residue 38 of Smk1, and the wild-type (WT) sample lacking Bpa are controls for cross-linking.

Table 1.

Yeast Strains

strain	genotype	source
JTY88	MAT**a**/MATα *ura3/ura3 leu2::hisG/leu2::hisG trp1::hisG/trp1::hisG lys2/lys2 ho::LYS2/ho::LYS2 SSP2ΔN161-GST::TRP1/ssp2Δ SMK1-HH::LEU2/SMK1*	this work
TPY11	MAT**a**/MATα *ura3/ura3 leu2::hisG/leu2::hisG trp1::hisG/trp1::hisG lys2/lys2 ho::LYS2/ho::LYS2 ssp2-ΔN137-F307A,F327A-GST::TRP1/ssp2Δ SMK1-HH::LEU2/SMK1*	this work
TPY12	MAT**a**/MATα *ura3/ura3 leu2::hisG/leu2::hisG trp1::hisG/trp1::hisG lys2/lys2 ho::LYS2/ho::LYS2 ssp2-ΔN137-GST::TRP1/ssp2Δ SMK1-HH::LEU2/SMK1*	this work
TPY13	MAT**a**/MATα *ura3/ura3 leu2::hisG/leu2::hisG trp1::hisG/trp1::hisG lys2/lys2 ho::LYS2/ho::LYS2 ssp2Δ/ssp2Δ SMK1-HH::LEU2/SMK1*	this work
TPY28	MAT**a**/MATα *ura3/ura3 leu2::hisG/leu2::hisG trp1::hisG/trp1::hisG lys2/lys2 ho::LYS2/ho::LYS2 ssp2-L2-GST::TRP1/ssp2Δ SMK1-HH::LEU2/SMK1*	this work
TPY29	MAT**a**/MATα *ura3/ura3 leu2::hisG/leu2::hisG trp1::hisG/trp1::hisG lys2/lys2 ho::LYS2/ho::LYS2 ssp2-L1-GST::TRP1/ssp2Δ SMK1-HH::LEU2/SMK1*	this work
TPY30	MAT**a**/MATα *ura3/ura3 leu2::hisG/leu2::hisG trp1::hisG/trp1::hisG lys2/lys2 ho::LYS2/ho::LYS2 ssp2-L3-GST::TRP1/ssp2Δ SMK1-HH::LEU2/SMK1*	this work
TPY36	MAT**a**/MATα *ura3/ura3 leu2::hisG/leu2::hisG trp1::hisG/trp1::hisG lys2/lys2 ho::LYS2/ho::LYS2 ssp2-L4-GST::TRP1/ssp2Δ SMK1-HH::LEU2/SMK1*	this work
JTY1016	MATa *pSSP2-SMK1–3XHA::KAN leu2-hisG trp1-hisG lys2 his4-N ura3 ho::LYS2*	this work
JTY1008	MATα *SMK1–8His-HA::Leu2 ssp2Δ ura3 trp1 his4-N lys2 ho::LYS2*	this work

Table 2.

Plasmids

plasmid	plasmid/insert(s)[a]	alias	source
pJT114	*pETDuet + SMK1 + GST*		24
pJT115	*pETDuet + SMK1 + SSP2$^{137–371}$-GST*	*SSP2-ΔN137-GST*	24
pJT118	*pETDuet + SMK1 + SSP2$^{162–371}$-GST*	*SSP2-ΔN161-GST*	24
pTP10	*pETDuet + SMK1-Y38TAG + SSP2$^{137–371}$-GST*		this work
pAR1	*pETDuet + SMK1 + SSP2$^{162–371}$-F211A-GST*		this work
pAR7	*pETDuet + SMK1 + SSP2$^{162–371}$-F327A-GST*		this work
pAR3	*pETDuet + SMK1 + SSP2$^{162–371}$-F211Y-GST*		this work
pAR4	*pETDuet + SMK1 + SSP2$^{162–371}$-F307A-GST*		this work
pAR6	*pETDuet + SMK1 + SSP2$^{162–371}$-F307Y-GST*		this work
pAR9	*pETDuet + SMK1 + SSP2$^{162–371}$-F327Y-GST*		this work
pAR10	*pETDuet + SMK1 + SSP2$^{162–371}$-F307A, F327A-GST*		this work
pAR11	*pETDuet + SMK1 + SSP2$^{162–371}$-F307Y, F327Y-GST*		this work
pTP14	*pETDuet + SMK1 + SSP2$^{266–371}$-GST*		this work
pTP15	*pETDuet + SMK1 + SSP2$^{282–371}$-GST*		this work
pTP27	*pETDuet + SMK1-I124TAG + SSP2$^{137–371}$-GST*		this work
pTP28	*pETDuet + SMK1-Y145TAG + SSP2$^{137–371}$-GST*		this work
pTP29	*pETDuet + SMK1-N171TAG + SSP2$^{137–371}$-GST*		this work
pTP30	*pETDuet + SMK1-L368TAG + SSP2$^{137–371}$-GST*		this work
pTP35	*pACYDuet-1 + MBP-SSP2$^{162–265CO}$*	MBP-KARL1	this work
pTP36	*pETDuet + SSP2$^{266–371}$-GST*	KARL2-GST	this work
pTP39	*pACYDuet-1 + MBP-SSP2$^{162–255CO}$*		this work
pTP40	*pACYDuet-1 + MBP-SSP2$^{162–245CO}$*		this work
pTP41	*pETDuet + SMK1 + SSP2$^{275–371}$-GST*		this work
pTP44	*pACYDuet-1 + MBP-SSP2$^{162–240CO}$*		this work
pTP45	*pACYDuet-1 + MBP-SSP2$^{162–235CO}$*		this work
pTP52	*pACYDuet-1 + MBP-SSP2$^{162–245CO}$*		this work
pTP53	*pETDuet + SMK1 + SSP2$^{137–371}$-R185TAG-GST*		this work

plasmid	plasmid/insert(s)[a]	alias	source
pTP54	*pETDuet + SMK1 + SSP2$^{137–37}$-Y195TAG-GST*		this work
pTP55	*pETDuet + SMK1 + SSP2$^{137–371}$-F211TAG-GST*		this work
pTP57	*pETDuet + SMK1 + SSP2$^{137-371}$-F229TAG-GST*		this work
pTP58	*pETDuet + SMK1 + SSP2$^{137–371}$-F307TAG-GST*		this work
pTP59	*pETDuet + SMK1 + SSP2$^{137–371}$-V317TAG-GST*		this work
pTP60	*pETDuet + SMK1 + SSP2$^{137–371}$-S324TAG-GST*		this work
pTP61	*pETDuet + SMK1 + SSP2$^{137–371}$-F327TAG-GST*		this work
pTP62	*pETDuet + SMK1 + SSP2$^{137–371}$-I330TAG-GST*		this work
pTP65	*pETDuet + SMK1-Y209TAG + SSP2$^{137–371}$-GST*		this work
pTP66	*pETDuet + SMK1 + SSP2$^{162–371}$-Δ247–256-GST*	*ssp2-L2*	this work
pTP67	*pETDuet + SMK1 + SSP2$^{162–371}$-2 × 247–256-GST*	*ssp2-L1*	this work
pTP68	*pETDuet + SMK1 + SSP2$^{162–371}$-Δ246–265::2xGGGS-GST*	*ssp2-L3*	this work
pTP69	*pETDuet + SMK1 + SSP2$^{162–371}$-Δ246–265::5xGGGS-GST*	*ssp2-L4*	this work
pTP70	*pETDuet + SMK1 + SSP2$^{162–371}$-Y223TAG-GST*		this work
pEVOL	P15A + tRNA synthetase/tRNA amber suppressor pair for incorporation of a Bpa photo-cross-linker		41

[a] A terminal superscript CO indicates DNA generated by in vitro gene synthesis that has been codon optimized for translation in *E. coli*.